AIAA JOURNAL
Vol. 33, No. 2, February 1995

Circular-Arc Inclusion at Isotropic Bimaterial Interface

C. K. Chao* and M. H. Shen*
National Taiwan Institute of Technology, Taipei, 106 Taiwan, Republic of China

A general solution to the circular-arc inclusion problem in bonded dissimilar media is provided. The proposed analysis is based on the use of Hilbert problem formulation, and a special technique of analytical continuation. The general expressions of the complex potentials are derived explicitly in both the circular inhomogeneity and the surrounding matrix. Several specific solutions are provided in closed form which are verified by comparison with existing ones. Numerical examples of composite materials under uniform remote load or a point force acting on the inclusion surface are examined and detailed results are presented. The oscillatory behavior in tractions along the interface is also discussed.

I. Introduction

THE characteristics of the stress field near the tip of a line inclusion have been extensively studied. A review on the related subject was given by Mura.[1] Based on the equivalent inclusion approach of Eshelby[2] and the complex variable method of Muskhelishvili,[3] Wang et al.[4] have considered the problem of a rigid line inhomogeneity in an isotropic elastic body under remote loading. They found analytical expressions of the corresponding elastic field and examined the characteristics of the resulting stress singularity. The same problem has also been considered by Erdogan and Gupta,[5] Atkinson,[6] and Ballarini,[7] among others. Based on Stroh[8] formalism for anisotropic elasticity, a line inclusion in an anisotropic elastic solid has been treated by Li and Ting.[9] Wu [10] studied a line inclusion at the interface of an anisotropic bimaterial and found that the near-tip stress field exhibits oscillatory singularities of the type $r^{-\frac{1}{2}\pm\gamma^*}$ with r being the distance measured from the tips of the line inclusion and γ^* a bimaterial constant. In Wu's paper,[10] the strain intensity factors are introduced to characterize the near-tip fields instead of using the stress singularity coefficients proposed by Wang et al.[4] All of the aforementioned investigators have concentrated on the plane problem of a line inclusion in an infinite medium. The corresponding problem associated with curvilinear inclusions has been rather limited. Recently, Chao and Shen[11] gave exact solutions of the elastic and thermoelastic problem with a rigid circular-arc inclusion. They showed that near-tip stress field exhibits a square-root singularity similar to the case of a traction-free crack.

In this paper, a circular-arc inclusion at an isotropic bimaterial interface is investigated. The Hilbert problem formulation and a special technique of analaytic continuation are employed to derive the stress and displacement fields in an explicit form. The general solution of the present problem is provided in Sec. II. The external loads considered in this study consist of a remote uniform load and concentrated force acting on the inclusion surface which are discussed separately in Sec. III and Sec. IV, respectively. In Sec. V, numerical examples for commonly used fiber reinforced composite such as carbon/aluminum and tungsten/aluminum systems are given to illustrate the use of the present approach. Finally, Sec. VI concludes the article.

II. Formulation and Solution of the Problem

Consider two homogeneous, isotropic elastic materials. Let one occupy the region S^+, interior to the unit circle, $r = 1$, whereas the other occupies the infinite region S^-, exterior to the unit circle, Fig. 1. The elastic properties of the material in S^+ can be specified by the constants μ_1 and κ_1 and those of the material S^- by μ_2 and κ_2 where μ_j are the shear modulus, and $\kappa_j = (3 - \nu_j)/(1 + \nu_j)$ for generalized plane stress and $\kappa_j = (3 - 4\nu_j)$ for plane strain with $\nu_j (j = 1.2)$ the Poisson's ratio. If the interface between the two materials contains a rigid-arc inclusion, then it can be represented as L and L^*, where L denotes the rigid-arc inclusion and L^* denotes the remaining part of the interface. The arc inclusion is denoted as $L = ab$, and $t = e^{i\varphi}$ are the point on the circle $|z| = 1$. In this problem, the applied load may cause a translation and rotation of the inclusion. It is assumed that the arc inclusion only rotates about its center by an angle ϵ by eliminating a rigid translation in the entire system. Then, the displacement vector of the rigid inclusion can be put in the form

$$V(t) = u + iv = i\epsilon t \qquad \text{on } L \tag{1}$$

To formulate the boundary value problem, the displacement will be specified on L whereas the continuity of the stresses and displacements are required on L^*, i.e.,

$$u_1^+ + iv_1^+ = V^+(t), \qquad \text{on } L \tag{2}$$

$$u_2^- + iv_2^- = V^-(t), \qquad \text{on } L \tag{3}$$

and

$$(\sigma_r)_1 + i(\tau_{r\theta})_1 = (\sigma_r)_2 + i(\tau_{r\theta})_2, \qquad \text{on } L^* \tag{4}$$

$$u_1 + iv_1 = u_2 + iv_2, \qquad \text{on } L^* \tag{5}$$

where the subscripts 1 and 2 stand for the physical quantities occupying in S^+ and S^-, respectively, and the superscripts + and − in Eqs. (2) and (3) are used to denote the boundary values of the displacement as they are approached from S^+ and S^-, respectively. For the two-dimensional theory of isotropic elasticity, the components of the stress and displacement can be expressed in terms of the complex functions $\Phi_j(z)$ and $\Psi_j(z)$. It follows[3]

$$(\sigma_r)_j + (\sigma_\theta)_j = 2[\Phi_j(z) + \overline{\Phi_j(z)}] \tag{6}$$

$$(\sigma_r)_j + i(\tau_{r\theta})_j = \Phi_j(z) + \overline{\Phi_j(z)} - z\overline{\phi_j'(z)} - \left(\frac{\bar{z}}{z}\right)\overline{\Psi_j(z)} \tag{7}$$

$$2\mu_j(u_j + iv_j) = \kappa_j\phi_j(z) - z\bar{\phi}_j'(\bar{z}) - \bar{\psi}_j(\bar{z}) \tag{8}$$

with

$$\phi_j'(z) = \Phi_j(z), \qquad \psi_j'(z) = \Psi_j(z) \qquad (j = 1, 2)$$

where the overbar denotes the conjugate of the complex function. To avoid having to consider directly the functions $\phi_j(z)$, $\psi_j(z)$, differentiating Eq. (8) with respect to φ, it gives

$$2\mu_j\left(\frac{\partial u_j}{\partial\varphi} + i\frac{\partial v_j}{\partial\varphi}\right) = iz\left[\kappa\Phi_j(z) - \overline{\Phi_j(z)} + \bar{z}\overline{\Phi_j'(z)} + \frac{\bar{z}}{z}\overline{\Psi_j(z)}\right] \tag{9}$$

Received Jan. 12, 1994; revision received July 12, 1994; accepted for publication July 18, 1994.

*Professor, Department of Mechanical Engineering.

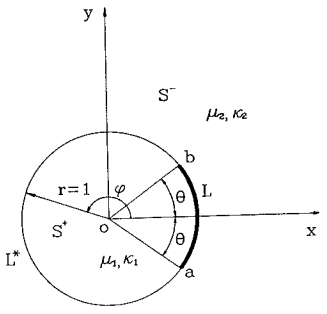

Fig. 1 Circular-arc inclusion on the interface of two isotropic materials.

For problems involving arcs of discontinuities, it is convenient to further introduce the functions[3]

$$\Omega_j(z) = \bar{\Phi}_j\left(\frac{1}{z}\right) - \frac{1}{z}\bar{\Phi}_j'\left(\frac{1}{z}\right) - \frac{1}{z^2}\bar{\Psi}_j\left(\frac{1}{z}\right), \qquad j = 1, 2 \quad (10)$$

Making use of Eqs. (9) and (10), Eqs. (2–5) can now be expressed in terms of $\Phi_j(z)$, $\Omega_j(z)$ as

$$\kappa_1\Phi_1^+(t) - \Omega_1^-(t) = 2\mu_1 V'^+(t), \qquad \text{on } L \quad (11)$$

$$\kappa_2\Phi_2^-(t) - \Omega_2^+(t) = 2\mu_2 V'^-(t), \qquad \text{on } L \quad (12)$$

and

$$\Phi_1(t) + \Omega_1(t) = \Phi_2(t) + \Omega_2(t), \qquad \text{on } L^* \quad (13)$$

$$\frac{1}{\mu_1}[\kappa_1\Phi_1(t) - \Omega_1(t)] = \frac{1}{\mu_2}[\kappa_2\Phi_2(t) - \Omega_2(t)], \qquad \text{on } L^* \quad (14)$$

Hence, a complete solution to the bimaterial inclusion problem has been reduced to the evaluation of four complex functions $\Phi_j(z)$, $\Omega_j(z)$, $(j = 1, 2)$, which must satisfy the conditions as given by Eqs. (11–14). A knowledge of the behavior of the complex functions for small and large values of $|z|$ is pertinent to the solutions of the dissimilar media problem. First of all, since $\Phi_1(z)$ and $\Psi_1(z)$ are holomorphic in S^+ they must take the forms

$$\Phi_1(z) = A_0 + A_1 z + A_2 z^2 + \cdots \qquad \text{for } |z| < 1 \quad (15)$$

$$\Psi_1(z) = B_0 + B_1 z + B_2 z^2 + \cdots \qquad \text{for } |z| < 1 \quad (16)$$

From Eqs. (10), (15), and (16), $\Omega_1(z)$ is found to be holomorphic in S^-. Therefore,

$$\Omega_1(z) = E_0 + \frac{E_1}{z} + \frac{E_2}{z^2}\cdots \qquad \text{for } |z| > 1 \quad (17)$$

where

$$E_0 = \bar{A}_0, \qquad E_1 = 0 \quad (18)$$

In the region S^-, $\Phi_2(z)$, and $\Psi_2(z)$ are holomorphic including the point at infinity, i.e.,

$$\Phi_2(z) = a_0 + \frac{a_1}{z} + \frac{a_2}{z} + \cdots \qquad \text{for } |z| > 1 \quad (19)$$

$$\Psi_2(z) = b_0 + \frac{b_1}{z} + \frac{b_2}{z^2} + \cdots \qquad \text{for } |z| > 1 \quad (20)$$

Substituting Eqs. (19) and (20) into Eq. (10) yields

$$\Omega_2(z) = -\frac{\bar{b}_0}{z^2} - \frac{\bar{b}_1}{z} + \xi(z) \qquad \text{for } |z| < 1 \quad (21)$$

which is holomorphic in S^+ with the exception of the point $z = 0$, and $\xi(z)$ is a polynomial in positive powers of z. The constants a_0, a_1 and b_0, b_1 appearing in Eqs. (19) and (20), respectively, can be found immediately by following the procedure described in Muskhelishvili[3] for the case of one material. If σ_1^∞ and σ_2^∞ denote the values of the principal stresses at infinity and ω the angle made by the direction of σ_1^∞ with the x axis, then

$$a_0 = \tfrac{1}{4}\left(\sigma_1^\infty + \sigma_2^\infty\right) + i\frac{2\mu_2\varepsilon^\infty}{1+\kappa_2} \quad (22)$$

$$b_0 = -\tfrac{1}{2}\left(\sigma_1^\infty - \sigma_2^\infty\right)e^{-2i\omega} \quad (23)$$

$$b_1 = \frac{\kappa_2(X - iY)}{2\pi(1+\kappa_2)} \quad (24)$$

where ε^∞ is the rotation at infinity, X and Y are the resultant forces acting on L, and a_1 is related to b_1 by $a_1 = -\bar{b}_1/\kappa_2$. To reduce the boundary problem to the solution of linear relationship or Hilbert problem, we must extend all complex functions $\Phi_j(z)$ and $\Omega_j(z)$ into the whole region. Starting from the assumptions that the stresses and displacements are continuous over the bonded segments of the circle $|z| = 1$, Eqs. (13) and (14) may be regarded as the conditions of analytic continuation of $\Phi_j(z)$ and $\Omega_j(z)$ from S^+ to S^- across L^*. Now, $\Phi_1(t)$ and $\Omega_1(t)$ in Eqs. (13) and (14) may be solved explicitly in terms of $\Phi_2(t)$ and $\Omega_2(t)$, and the resulting expressions are valid everywhere in the z plane as

$$\Phi_1(z) = \frac{\mu_2 + \mu_1\kappa_2}{\mu_2(1+\kappa_1)}\Phi_2(z) + \frac{\mu_2 - \mu_1}{\mu_2(1+\kappa_1)}\Omega_2(z) \quad (25)$$

$$\Omega_1(z) = \frac{\mu_2\kappa_1 - \mu_1\kappa_2}{\mu_2(1+\kappa_1)}\Phi_2(z) + \frac{\mu_1 + \mu_2\kappa_1}{\mu_2(1+\kappa_1)}\Omega_2(z) \quad (26)$$

Substituting Eqs. (15) and (21) into Eq. (25), the definition of the function $\Phi_2(z)$ can be extended into the region S^+ by allowing poles up to the second order at $z = 0$. This gives

$$\Phi_2(z) = \frac{T_1}{z^2} + \frac{T_2}{z} + \eta(z) \qquad \text{for } |z| < 1 \quad (27)$$

where $\eta(z)$ is a function holomorphic everywhere in the region S^+, and

$$T_1 = \frac{\mu_2 - \mu_1}{\mu_2 + \mu_1\kappa_2}\bar{b}_0, \qquad T_2 = \frac{\mu_2 - \mu_1}{\mu_2 + \mu_1\kappa_2}\bar{b}_1 \quad (28)$$

Similarly, substituting Eqs. (17) and (19) into Eq. (26), the function $\Omega_2(z)$ can also be extended into the region $|z| > 1$ as

$$\Omega_2(z) = \zeta(z) \quad (29)$$

where $\zeta(z)$ is a holomorphic function everywhere in S^-. Inserting Eqs. (25) and (26) into the boundary conditions Eqs. (11) and (12) and solving them simultaneously yields

$$\left[\Phi_2(t) - \frac{1}{\kappa_2}\Omega_2(t)\right]^+ + \frac{\kappa_2}{\kappa_1}\alpha\left[\Phi_2(t) - \frac{1}{\kappa_2}\Omega_2(t)\right]^- = f(t) \quad (30)$$

$$\left[\Phi_2(t) + \frac{\alpha}{\kappa_1}\Omega_2(t)\right]^+ - \left[\Phi_2(t) + \frac{\alpha}{\kappa_1}\Omega_2(t)\right]^- = g(t) \quad (31)$$

where

$$f(t) = \frac{2\kappa_2\mu_1\mu_2(1+\kappa_1)V'^+(t) + 2\kappa_1\mu_2^2(1+\kappa_2)V'^-(t)}{\kappa_1\kappa_2(\mu_2 + \mu_1\kappa_2)} \quad (32)$$

$$g(t) = \frac{2\mu_1\mu_2(1+\kappa_1)[V'^+(t) - V'^-(t)]}{\kappa_1(\mu_2 + \mu_1\kappa_2)} \quad (33)$$

Since in this problem $V'^+(t) = V'^-(t) = \epsilon i$, Eqs. (32) and (33) become

$$f(t) = 2i\epsilon m_1 \quad (34)$$

$$g(t) = 0 \quad (35)$$

where

$$m_1 = \frac{\kappa_2\mu_1\mu_2(1+\kappa_1) + \kappa_1\mu_2^2(1+\kappa_2)}{\kappa_1\kappa_2(\mu_2 + \mu_1\kappa_2)} \quad (36)$$

and they must satisfy the Hölder condition on L. The parameter α appearing in Eqs. (30) and (31) stands for

$$\alpha = \frac{\mu_1 + \mu_2\kappa_1}{\mu_2 + \mu_1\kappa_2}$$

Knowing that Eq. (31) is a Plemelj equation for the function $\Phi_2(z) + (\alpha/\kappa_1)\Omega_2(z)$, and using the properties from Eqs. (21) and (27), we have

$$\Phi_2(z) + \frac{\alpha}{\kappa_1}\Omega_2(z) = e_0 + \frac{t_2}{z} + \frac{t_1}{z^2} \tag{37}$$

Furthermore, the nonhomogeneous Hilbert equation (30) gives

$$\Phi_2(z) - \frac{1}{\kappa_2}\Omega_2(z) = \frac{X(z)}{2\pi i}\int_L \frac{2i\epsilon m_1}{X^+(t)(t-z)}\,dt + X(z)\left[c_0 + c_1 z + \frac{D_1}{z} + \frac{D_2}{z^2}\right] \tag{38}$$

where the Plemelj function

$$X(z) = (z-a)^{-\frac{1}{2}+i\beta}(z-b)^{-\frac{1}{2}-i\beta} \tag{39}$$

The exponent β appearing in Eq. (39) is

$$\beta = \frac{1}{2\pi}\log\left(\frac{\kappa_2}{\kappa_1}\alpha\right)$$

which is referred to as a bielastic constant. It is noted that singularities of the stress field near the arc inclusion tip are the same as those for the corresponding line inclusion problem.[12]

By means of Eqs. (25), (26), (37), and (38), the general solution involving the four unknown functions $\Phi_j(z)$, $\Omega_j(z)$, $(j = 1, 2)$, may be arranged into a compact form as follows:

$$\Phi_1(z) = H_1F_1(z) + H_2F_2(z) \tag{40}$$

$$\Omega_1(z) = H_3F_1(z) + H_4F_2(z) \tag{41}$$

and

$$\Phi_2(z) = \frac{\kappa_2(\mu_1 + \mu_2\kappa_1)F_1(z) + \kappa_1(\mu_2 + \mu_1\kappa_2)F_2(z)}{\kappa_2(\mu_1 + \mu_2\kappa_1) + \kappa_1(\mu_2 + \mu_1\kappa_2)} \tag{42}$$

$$\Omega_2(z) = \frac{\kappa_1\kappa_2(\mu_2 + \mu_1\kappa_2)}{\kappa_2(\mu_1 + \mu_2\kappa_1) + \kappa_1(\mu_2 + \mu_1\kappa_2)}[F_2(z) - F_1(z)] \tag{43}$$

where

$$F_1(z) = \frac{X(z)}{2\pi i}\int_L \frac{2i\epsilon m_1}{X^+(t)(t-z)}\,dt + X(z)\left[c_0 + c_1 z + \frac{D_1}{z} + \frac{D_2}{z^2}\right] \tag{44}$$

$$F_2(z) = e_0 + \frac{t_2}{z} + \frac{t_1}{z^2} \tag{45}$$

and

$$H_1 = \frac{\kappa_2(\mu_1 + \mu_2\kappa_1)(\mu_2 + \mu_1\kappa_2)}{\mu_2(1+\kappa_1)[\kappa_2(\mu_1 + \mu_2\kappa_1) + \kappa_1(\mu_2 + \mu_1\kappa_2)]} - \frac{\kappa_1\kappa_2(\mu_2 - \mu_1)(\mu_2 + \mu_1\kappa_2)}{\mu_2(1+\kappa_1)[\kappa_2(\mu_1 + \mu_2\kappa_1) + \kappa_1(\mu_2 + \mu_1\kappa_2)]}$$

$$H_2 = \frac{\kappa_1(\mu_2 + \mu_1\kappa_2)^2 + \kappa_1\kappa_2(\mu_2 - \mu_1)(\mu_2 + \mu_1\kappa_2)}{\mu_2(1+\kappa_1)[\kappa_2(\mu_1 + \mu_2\kappa_1) + \kappa_1(\mu_2 + \mu_1\kappa_2)]}$$

$$H_3 = \frac{\kappa_2(\mu_1 + \mu_2\kappa_1)(\mu_2\kappa_1 - \mu_1\kappa_2)}{\mu_2(1+\kappa_1)[\kappa_2(\mu_1 + \mu_2\kappa_1) + \kappa_1(\mu_2 + \mu_1\kappa_2)]} - \frac{\kappa_1\kappa_2(\mu_1 + \mu_2\kappa_1)(\mu_2 + \mu_1\kappa_2)}{\mu_2(1+\kappa_1)[\kappa_2(\mu_1 + \mu_2\kappa_1) + \kappa_1(\mu_2 + \mu_1\kappa_2)]}$$

$$H_4 = \frac{\kappa_1(\mu_2 + \mu_1\kappa_2)(\mu_2\kappa_1 - \mu_1\kappa_2)}{\mu_2(1+\kappa_1)[\kappa_2(\mu_1 + \mu_2\kappa_1) + \kappa_1(\mu_2 + \mu_1\kappa_2)]} + \frac{\kappa_1\kappa_2(\mu_1 + \mu_2\kappa_1)(\mu_2 + \mu_1\kappa_2)}{\mu_2(1+\kappa_1)[\kappa_2(\mu_1 + \mu_2\kappa_1) + \kappa_1(\mu_2 + \mu_1\kappa_2)]}$$

The line integral appearing in Eq. (44) can be evaluated by residual theory, and the result is

$$\frac{X(z)}{2\pi i}\int_L \frac{2i\epsilon m_1}{X^+(t)(t-z)}\,dt = \frac{2m_1\epsilon i}{1 + \frac{\kappa_2}{\kappa_1}\alpha}[1 - (z - \cos\theta + 2\beta\sin\theta)X(z)] \tag{46}$$

The quantities t_1 and t_2 in Eq. (37) may be associated with the coefficients of the series given by Eqs. (21) and (27) as

$$t_1 = T_1 - \frac{\alpha}{\kappa_1}\bar{b}_0 \qquad t_2 = T_2 - \frac{\alpha}{\kappa_1}\bar{b}_1 \tag{47}$$

$$t_1 = \frac{\mu_1(1+\kappa_1)}{\kappa_1(\mu_2 + \mu_1\kappa_2)}\bar{b}_0, \qquad t_2 = -\frac{\mu_1(1+\kappa_1)}{\kappa_2(\mu_2 + \mu_1\kappa_2)}\bar{b}_1 \tag{48}$$

Using the behavior of the stress function $\Phi_2(z) - (1/\kappa_2)\Omega_2(z)$ near the point $|z| = 0$ and applying Eq. (46), there follows

$$X(z)\left(\frac{D_1}{z} + \frac{D_2}{z^2}\right) = \frac{T_1 + (\bar{b}_0/\kappa_2)}{z^2} + \frac{T_2 + (\bar{b}_1/\kappa_2)}{z} \tag{49}$$

In addition, the constants e_0, c_0, and c_1 may be determined by applying the behavior of the stress functions $\Phi_2(z)$ for large values of $|z|$ in conjunction with Eq. (18). Now, we have completed the general solution to the given problem once the rotation angle ϵ is determined such that the resultant moment of the force, acting on the inclusion from the surrounding material, must vanish. In the following work, two different loading cases are considered to illustrate the use of the present approach.

III. Uniaxial Tension at Infinity

As an application to the theory, consider an uniform load p directed at an angle ω applying at infinity and no resultant force acting on the rigid inclusion. It implies

$$a_0 = \frac{p}{4}, \qquad b_0 = -\frac{p}{2}e^{-2i\omega}, \qquad a_1 = b_1 = 0$$

Referring to Fig. 2, the circular-arc inclusion subtends an angle of 2θ symmetrically with the positive $x$axis. The ends of the cut L are located at $a = \exp(-i\theta)$ and $b = \exp(i\theta)$ on $|z| = 1$. Hence, Eq. (39) becomes

$$X(z) = (z - e^{-i\theta})^{-\frac{1}{2}+i\beta}(z - e^{-i\theta})^{-\frac{1}{2}-i\beta} \tag{50}$$

Expanding Eq. (50) near $z = 0$ renders

$$X(z) = -e^{2\beta\theta}\left[1 + M_1 z + M_2 z^2 + \cdots\right] \tag{51}$$

where

$$M_1 = \cos\theta + 2\beta\sin\theta$$

$$M_2 = \frac{3\cos 2\theta + 1}{4} + \beta^2(1 - \cos\theta) + 2\beta\sin 2\theta$$

The constants D_1 and D_2 can be obtained in a straightforward manner from Eq. (49). The results are

$$D_2 = e^{-2\beta\theta}\frac{\mu_2 + \mu_2\kappa_2}{\kappa_2(\mu_2 + \mu_1\kappa_2)}\frac{p}{2}e^{2i\omega} \tag{52}$$

$$D_1 = -M_1 e^{-2\beta\theta}\frac{\mu_2 + \mu_2\kappa_2}{\kappa_2(\mu_2 + \mu_1\kappa_2)}\frac{p}{2}e^{2i\omega} \tag{53}$$

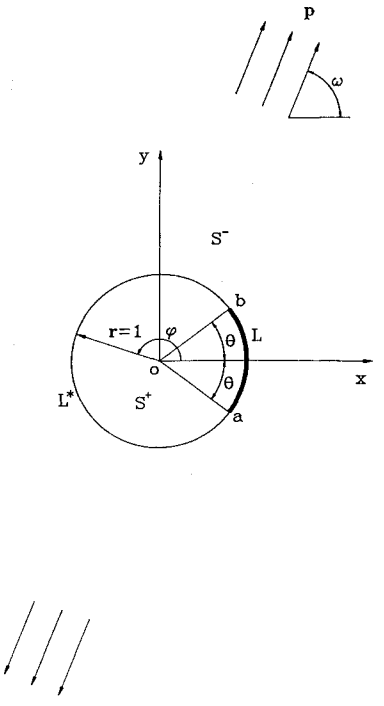

Fig. 2 Circular-arc inclusion in bonded dissimilar materials under uniform remote load.

Now, the supplementary condition equivalent to Eqs. (15), (17), and (18) gives

$$\Phi_1(0) = \bar{\Omega}_1, (\infty) \tag{54}$$

Inserting Eqs. (40) and (41) into Eq. (54) and using the property of $X(z)$ for large $|z|$

$$X(z) = \frac{1}{z} + \frac{N_1}{z^2} + \cdots \qquad \text{for } |z| > 1$$

where

$$N_1 = \cos\theta - 2\beta \sin\theta$$

yield the following equation:

$$H_3 c_1 + H_4 e_0 = H_1\left[Gi - e^{2\beta\theta}(\bar{c}_0 + M_1\bar{D}_1 + M_2\bar{D}_2)\right] + H_2\bar{e}_0 \tag{55}$$

where

$$G = \frac{-2m_1\epsilon}{1 + (\kappa_2/\kappa_1)\alpha}[1 + e^{2\beta\theta}(-\cos\theta + 2\beta\sin\theta)]$$

Furthermore, as $|z| \to \infty$

$$\Phi_2(z) \to \frac{p}{4} + O\left(\frac{1}{z^2}\right) \tag{56}$$

Putting Eq. (42) into Eq. (56) and using the property with the knowledge that for large $|z|$

$$\frac{X(z)}{2\pi i}\int_L \frac{2i\epsilon m_1}{X^+(t)(t-z)}\,dt \to O\left(\frac{1}{z^2}\right)$$

yield the following equations

$$c_0 + N_1 c_1 = 0 \tag{57}$$

$$\frac{\kappa_2(\mu_1 + \mu_2\kappa_1)c_1 + \kappa_1(\mu_2 + \mu_1\kappa_2)e_0}{\kappa_2(\mu_1 + \mu_2\kappa_1) + \kappa_1(\mu_2 + \mu_1\kappa_2)} = \frac{p}{4} \tag{58}$$

After some algebraic manipulations, the final explicit forms are obtained as

$$c_1 = \frac{-H_1\kappa_1(\mu_2+\mu_1\kappa_2)e^{2\beta\theta}(M_1\mathcal{R}[D_1] + M_2\mathrm{Re}[D_2])}{\kappa_1(\mu_2+\mu_1\kappa_2)\left(H_3 - H_1e^{2\beta\theta}N_1\right) + \kappa_2(\mu_1+\mu_2\kappa_1)(H_2-H_4)}$$
$$+ \frac{p/4(H_2-H_4)[\kappa_2(\mu_1+\mu_2\kappa_1) + \kappa_1(\mu_2+\mu_1\kappa_2)]}{\kappa_1(\mu_2+\mu_1\kappa_2)\left(H_3 - H_1e^{2\beta\theta}N_1\right) + \kappa_2(\mu_1+\mu_2\kappa_1)(H_2-H_4)}$$
$$+ i\frac{\kappa_1(\mu_2+\mu_1\kappa_2)H_1\left[G + e^{2\beta\theta}(M_1\mathrm{Im}[D_1] + M_2\mathrm{Im}[D_2])\right]}{\kappa_1(\mu_2+\mu_1\kappa_2)\left(H_3 + H_1e^{2\beta\theta}N_1\right) - \kappa_2(\mu_1+\mu_2\kappa_1)(H_2+H_4)} \tag{59}$$

$$c_0 = -N_1 c_1 \tag{60}$$

$$e_0 = \frac{p}{4}\left[\frac{\kappa_2(\mu_1 + \mu_2\kappa_1)}{\kappa_1(\mu_2 + \mu_1\kappa_2)} + 1\right] - \frac{\kappa_2(\mu_1 + \mu_2\kappa_1)}{\kappa_1(\mu_2 + \mu_1\kappa_2)}c_1 \tag{61}$$

where Re and Im denote the real and imaginary part of the complex functions, respectively.

There remains the determination of the angle ϵ from the condition that the resultant moment of the forces, acting on the inclusion from the surrounding material, must vanish. The formula for this moment was first given by Muskhelishvili[3]

$$M = -Re\left[\int \psi_j(z)\,dz - z\psi_j(z) - z\bar{z}\phi_j(z)\right]_C \tag{62}$$

where the contour around the rigid inclusion C is taken in a clockwise direction. Since in the present case $\phi_2(z)$ and $\psi_2(z)$ are single valued in S^-, the resultant moment M_0 about the origin becomes

$$M_0 = Re\left[\int \psi_2(z)\,dz\right]_C \tag{63}$$

Applying Eq. (63) and replacing C by a circle at a large distance from the origin, one can have $\Psi_2(z)$ for large $|z|$ the form

$$\Psi_2(z) = b_0 + \frac{b_1}{z} + \frac{iM_0 + N}{2\pi}\frac{1}{z^2} + O\left(\frac{1}{z^3}\right) \tag{64}$$

where N is a real constant. Substituting Eq. (64) into Eq. (10), $\Omega_2(z)$ near $|z| = 0$ has the form

$$\Omega_2(z) = -\frac{\bar{b}_0}{z^2} - \frac{\bar{b}_1}{z} + \left(\frac{-M_0 i + N}{2\pi} + \bar{a}_0\right)O(z) \qquad \text{for } |z| < 1 \tag{65}$$

Inserting all coefficients into Eq. (43) and comparing Eqs. (43) and (65), one has

$$M_0 = \frac{2\pi\kappa_1\kappa_2(\mu_2 - \mu_1\kappa_2)}{\kappa_2(\mu_1 - \mu_2\kappa_1) + \kappa_1(\mu_2 + \mu_1\kappa_2)}\left\{\frac{2m_1\epsilon}{1 + (\kappa_2/\kappa_1)\alpha}\right.$$
$$\times [1 + e^{2\beta\theta}(-\cos\theta + 2\beta\sin\theta)] - e^{2\beta\theta}(\mathrm{Im}[c_0] + M_1\mathrm{Im}[D_1]$$
$$\left. + M_2\mathrm{Im}[D_2]) - \mathrm{Im}[e_0]\right\} \tag{66}$$

By putting $M_0 = 0$, we have a equation for ϵ. Now, all of the coefficients appearing in Eqs. (37) and (38) are solved and the results constitute a closed-form solution to the given problem. Consider a special case when both the unit disk and the surrounding medium are of the same material, the angle ϵ from Eq. (66) can be obtained in an explicit form

$$\epsilon = \frac{-p\sin^2\theta\sin 2\omega}{8\mu(1 - \cos\theta)} \tag{67}$$

For the limiting case of a small inclusion ($\theta \to 0$), Eq. (67) further reduces to

$$\epsilon = \frac{-p \sin 2\omega}{4\mu} \tag{68}$$

which is in agreement with the result of a straight inclusion given by Muskhelishvili.[3]

To examine the magnitude of the local stress field, the complex stress singularity coefficients are computed in the present study. In this work, the complex stress singularity coefficients at point b are defined as

$$S_I - iS_{II} = \sqrt{2\pi} \lim_{z \to e^{i\theta}} (z - e^{i\theta})^{\frac{1}{2}+i\beta}(\sigma_r + i\tau_{r\theta}), \qquad z \in L^* \tag{69}$$

Note that the definition of the stress singularity coefficients presented previously is different from that for line inclusion problem given by Wang et al.[4] In their paper, the stress singularity coefficients associated with mode II deformation is calculated from a tensile load which is applied parallel to the line inhomogeneity. Substituting Eq. (7) into Eq. (69), the complex stress singularity coefficients are

$$\begin{aligned} S_I - iS_{II} = {} & \frac{-\sqrt{\pi}\mu_1\kappa_2(1-\kappa_1\kappa_2)}{\kappa_2(\mu_1+\mu_2\kappa_1)+\kappa_1(\mu_2+\mu_1\kappa_2)]\sqrt{\sin\theta}} \\ & \times \frac{\exp(\{\beta(\theta+\pi)+i[(\pi/2)-(\theta/2)+\beta\log(2\sin\theta)]\})}{\kappa_2(\mu_1+\mu_2\kappa_1)+\kappa_1(\mu_2+\mu_1\kappa_2)]\sqrt{\sin\theta}} \\ & \times \left\{ \frac{2m_1\epsilon}{1+(\kappa_2/\kappa_1)\alpha}(1-2\beta i)\sin\theta \right. \\ & \left. + c_0 + c_1 e^{i\theta} + D_1 e^{-i\theta} + D_2 e^{-2i\theta} \right\} \end{aligned} \tag{70}$$

For a limiting case of homogeneous material, Eq. (70) becomes

$$\begin{aligned} S_I - iS_{II} = {} & \frac{\sqrt{\pi}[(\kappa-1)/2][\sin(\theta/2)+i\cos(\theta/2)]}{\kappa\sqrt{\sin\theta}} \\ & \times \left[\frac{-p\sin^3\theta\sin 2\omega}{4(1-\cos\theta)} + d_1 i\sin\theta \right. \\ & \left. - \frac{pe^{2i\omega}\cos\theta e^{-i\theta}}{2} + \frac{pe^{2i\omega}e^{-2i\theta}}{2} \right] \end{aligned} \tag{71}$$

where

$$d_1 = \frac{2p(\kappa-\kappa^2)+p\sin^2\theta\cos 2\omega}{4(1-\cos\theta-2\kappa)}$$

Consider a special case of small arc angle θ and $\omega = 0$ deg, Eq. (71) further reduces to

$$S_I = \frac{(3-\kappa)p}{8\kappa}(\kappa-1)\sqrt{\pi\theta}, \qquad S_{II} = 0 \tag{72}$$

It is seen that the mode I stress coefficient coincides with the result given by Wang et al.[4]

IV. Concentrated Force Applying on the Rigid Inclusion

Consider another case of loading condition that a concentrated force $F_x + iF_y$ applies on the inclusion at $z = e^{i\delta}$, ($|\delta| < \theta$), whereas the stress is zero at infinity (Fig. 3). This implies

$$a_0 = b_0 = 0, \qquad a_1 = -\frac{F_x + iF_y}{2\pi(1+\kappa_2)}$$

$$b_1 = -\frac{\kappa_2(F_x - iF_y)}{2\pi(1+\kappa_2)}$$

Analogous to the preceding procedures, all coefficients in Eqs. (37) and (38) are given as

$$D_1 = -e^{-2\beta\theta}\frac{(\mu_2+\mu_2\kappa_2)(F_x+iF_y)}{2\pi(\mu_2+\mu_1\kappa_2)(1+\kappa_2)} \tag{73}$$

$$D_2 = 0 \tag{74}$$

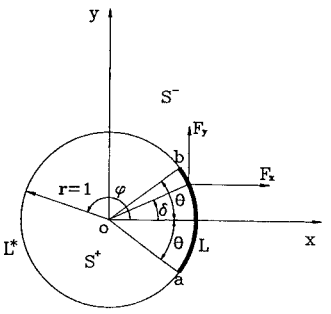

Fig. 3 Circular-arc inclusion in bonded dissimilar materials under concentrated force acting on the inclusion surface.

$$\begin{aligned} c_1 = {} & \frac{-H_1\kappa_1(\mu_2+\mu_1\kappa_2)e^{2\beta\theta}(\mathrm{Re}[R]+M_1\mathrm{Re}[D_1])}{\kappa_1(\mu_2+\mu_1\kappa_2)\left(H_3-H_1e^{2\beta\theta}N_1\right)+\kappa_2(\mu_1+\mu_2\kappa_1)(H_2-H_4)} \\ & + i\frac{\kappa_1(\mu_2+\mu_1\kappa_2)H_1\left[G+e^{2\beta\theta}(-\mathrm{Im}[R]+M_1\mathrm{Im}[D_1])\right]}{\kappa_1(\mu_2+\mu_1\kappa_2)\left(H_3-H_1e^{2\beta\theta}N_1\right)-\kappa_2(\mu_1+\mu_2\kappa_1)(H_2+H_4)} \end{aligned} \tag{75}$$

$$c_0 = -N_1c_1 - R \tag{76}$$

$$e_0 = -\frac{\kappa_2(\mu_1+\mu_2\kappa_1)}{\kappa_1(\mu_2+\mu_1\kappa_2)}c_1 \tag{77}$$

where

$$R = \frac{\mu_2\kappa_1}{2\pi\kappa_2(\mu_1+\mu_2\kappa_1)}(F_x+iF_y)$$

From Eq. (63), the resultant moment of the forces acting on the inclusion can be obtained as

$$\begin{aligned} M_0 = {} & \frac{2\pi\kappa_1\kappa_2(\mu_2+\mu_1\kappa_2)}{\kappa_2(\mu_1+\mu_2\kappa_1)+\kappa_1(\mu_2+\mu_1\kappa_2)} \\ & \times \left\{ \frac{2m_1\epsilon}{1+(\kappa_2/\kappa_1)\alpha}[1+e^{2\beta\theta}(-\cos\theta+2\beta\sin\theta)] \right. \\ & \left. - e^{2\beta\theta}\mathrm{Im}[c_0]+M_1\mathrm{Im}[D_1]-\mathrm{Im}[e_0] \right\} \end{aligned} \tag{78}$$

By putting $M_0 = F_y\sin\delta - F_x\cos\delta$, the rotation ϵ can be found from Eq. (77), and then the problem is solved. Consider a special case of homogeneous material, the rotation angle can be obtained in an explicit form

$$\epsilon = \frac{(F_y\cos\delta - F_x\sin\delta)(1-\cos\theta+2\kappa) - \kappa F_y(1+\cos\theta)}{4\pi\mu(1-\cos\theta)(1+\kappa)} \tag{79}$$

It is understood that the angle ϵ vanishes when the inclusion is under symmetric loading, i.e., $F_y = 0$ and $\delta = 0$. Following the previous procedures, the stress singularity coefficients can also be obtained by substituting Eqs. (73–77) into Eq. (70). For a special case of homogeneous material, the stress singularity coefficients at point b are found to be

$$\begin{aligned} S_I - iS_{II} = {} & \frac{\sqrt{\pi}\dfrac{(\kappa-1)}{2}[\sin(\theta/2)+i\cos(\theta/2)]}{\kappa\sqrt{\sin\theta}} \\ & \times \left\{ \frac{\sin\theta(F_y\cos\delta - F_x\sin\delta)(1-\cos\theta+2\kappa)}{2\pi(1-\cos\theta)(1+\kappa)} \right. \\ & - \frac{\sin\theta[\kappa F_y(1+\cos\theta)]}{2\pi(1-\cos\theta)(1+\kappa)} + d_2 i\sin\theta \\ & \left. - \frac{\kappa(F_x+iF_y)}{2\pi(1+\kappa)}(1+e^{-i\theta}) \right\} \end{aligned} \tag{80}$$

where

$$d_2 = \frac{\kappa F_x(1+\cos\theta)}{2\pi(1+\kappa)(1-\cos\theta-2\kappa)} + i\frac{(F_y\cos\delta - F_x\sin\delta)}{2\pi(1+\kappa)}$$

Consider the case of symmetric loading, i.e., $F_y = 0$ and $\delta = 0$, the stress singularity coefficients in Eq. (80) further reduce to

$$S_{\mathrm{I}} - iS_{\mathrm{II}} = \frac{(1-\kappa)F_x}{4(1+\kappa)\sqrt{\pi\sin\theta}}\left\{\left[\frac{2(1-\kappa)}{1-\cos\theta-2\kappa}\sin\theta\cos\frac{\theta}{2} + (1+\cos\theta)\sin\frac{\theta}{2}\right] - \left[\frac{2(1-\kappa)}{1-\cos\theta-2\kappa}\sin\theta\sin\frac{\theta}{2} - (1+\cos\theta)\cos\frac{\theta}{2}\right]i\right\}$$

It is interesting to note that the mode I stress singularity coefficient S_{I} always takes to be negative value for any material property $1 < \kappa < 3$ as the force F_x is applied on the rigid inclusion in the direction away from the fiber.

V. Numerical Examples

To illustrate the solutions derived in the previous sections for the fundamental nature of the circular-arc inclusion problem in bonded dissimilar media, two typical examples of composite materials under remote uniform load or concentrated force applied on a rigid inclusion are considered in this article. Let the material of the surrounding matrix be aluminum and the fiber be carbon or tungsten whose material properties are listed in Table 1.

The rotation angle ϵ of a rigid inclusion due to remote uniform load for carbon/aluminum and tungsten/aluminum composites can be determined from Eq. (66) and illustrated in Fig. 4. It is realized that carbon/aluminum composite experiences much larger rotation angle as compared to tungsten/aluminum composite since the fiber of tungsten/aluminum composite is made more rigid than that of carbon/aluminum composite. Similar observations can also be found for the case of concentrated force F_x applied on a rigid inclusion, Fig. 5. The tractions along the interface for tungsten/aluminum composite and carbon/aluminum composite are shown in Figs. 6 and 7, respectively, with half-inclusion angle $\theta = 50$ deg and $\omega = 0$ deg.

Table 1 Typical properties of materials for composites

	Fiber		Matrix
Properties	Carbon	Tungsten	Aluminum
Shear modulus, GN/m^2	82.8	165.6	27.2
Poisson's ratio	0.2	0.3	0.33
Composites	Carbon/aluminum		Tungsten/aluminum
Oscillatory index β	−0.068		−0.067

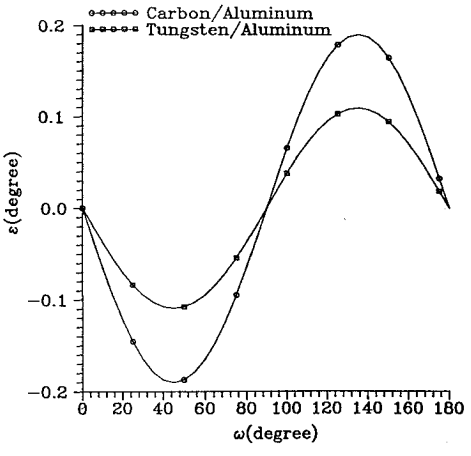

Fig. 4 Rotation angle vs load angle ω under remote uniform load p = 1 N/m^2 with half-inclusion angle θ = 50 deg.

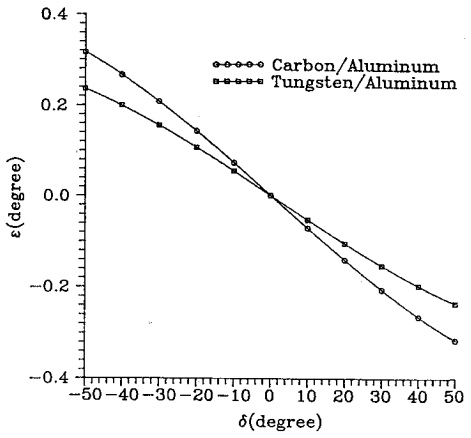

Fig. 5 Rotation angle vs load angle δ under concentrated force F_x = 1 Nm with half-inclusion angle θ = 50 deg.

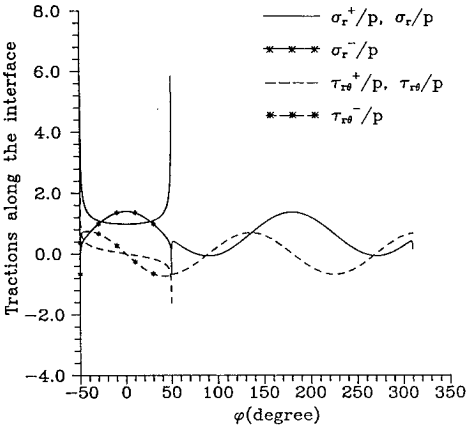

Fig. 6 Interface tractions for tungsten/aluminum composite with load angle ω = 0 deg and half-inclusion angle θ = 50 deg.

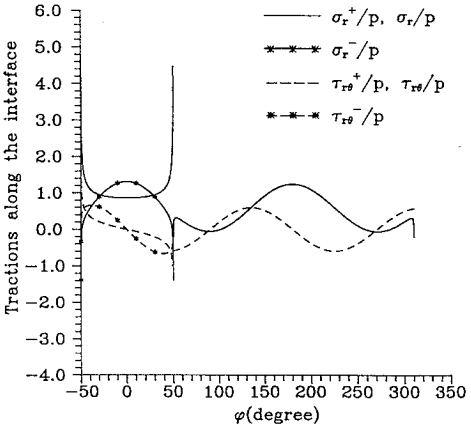

Fig. 7 Interface tractions for carbon/aluminum composite with load angle ω = 0 deg and half-inclusion angle θ = 50 deg.

The dash and solid lines denote the shear and radial stresses, respectively, and star symbols stand for the stresses on the outer side of the inclusion surface. The results show that the magnitude of interface tractions increases with the rigidity of the fiber. It is interesting to note that a negatively singular traction σ_r around the inclusion tips occurs in both the bonded interface and the outer side of the inclusion surface for each composite material whereas a positively singular traction σ_r is found to occur along the inner side of the inclusion surface. However, the trend is reversed if the load angle shifts from $\omega = 0$ deg to $\omega = 90$ deg at which a positively singular

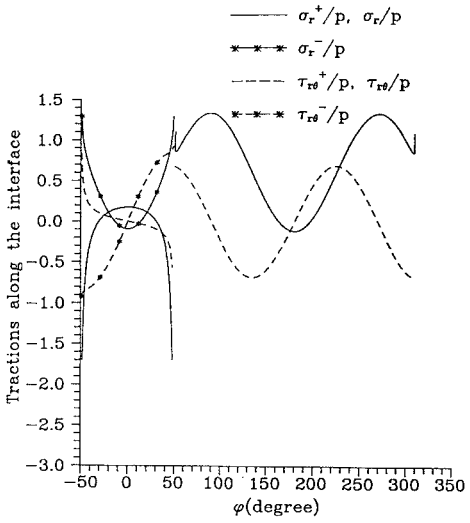

Fig. 8 Interface tractions for tungsten/aluminum composite with load angle ω = 90 deg and half-inclusion angle θ = 50 deg.

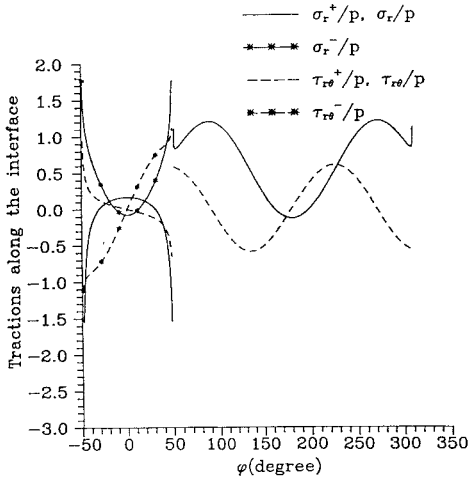

Fig. 9 Interface tractions for carbon/aluminum composite with load angle ω = 90 deg and half-inclusion angle θ = 50 deg.

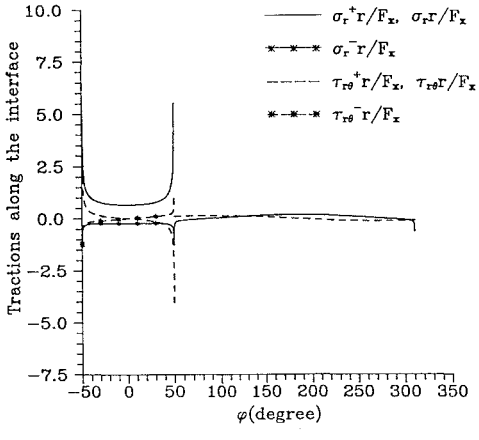

Fig. 10 Interface tractions for tungsten/aluminum composite with load angle δ = 0 deg and half-inclusion angle θ = 50 deg.

traction σ_r prevails along both the bonded interface and the outer side of the inclusion surface as indicated in Figs. 8 and 9. It must be emphasized that the strength of a positively singular traction on the inclusion surface is higher than that on the bonded interface. This predicts that, depending on the load angle, either matrix splitting or fiber splitting would occur along the inclusion surface as consider

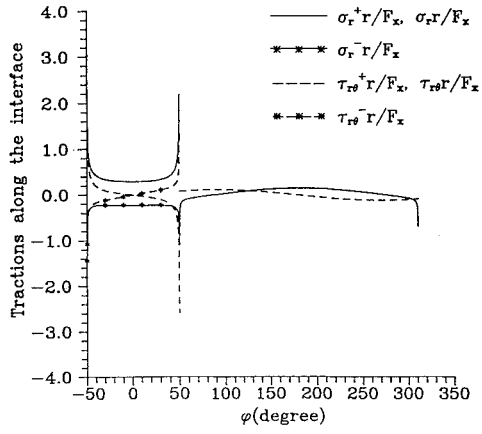

Fig. 11 Interface tractions for carbon/aluminum composite with load angle δ = 0 deg and half-inclusion angle θ = 50 deg.

in the present study. Similar phenomena can also be seen for the case when the force F_x is applied on the rigid inclusion at its central point ($\delta = 0$ deg) in the direction away from the fiber as are shown in Figs. 10 and 11. Consequently, it would lead to fiber splitting along the inclusion surface if the sufficient force F_x is applied on the rigid inclusion. Note that, based on dimensional analysis, the magnitude of interface tractions is inversely proportional to the radius of the fiber when the force applied on the inclusion is kept to be constant. Another interesting aspect is that the oscillatory behavior in tractions does not appear clearly in Figs. 6–11 inclusive. Referring to Eq. (39), the oscillation is represented in $\rho^{-\frac{1}{2}+i\beta}$ or $\cos(\beta \ln \rho) \pm i \sin(\beta \ln \rho)$, where ρ is the distance ahead or behind of the inclusion tip. That is, if $\beta \ln \rho$ change 2π then the traction will be able to have a cycle of oscillation. Referring to Table 1, the oscillation index β is so small that ρ must have the order of 10^{-40} to make the argument $\beta \ln \rho$ to increase or decrease 2π. This scale is far beyond the assumption of the classical continuum mechanics.

VI. Conclusion

A general solution for the interface circular-arc inclusion between dissimilar isotropic materials has been obtained by applying the Hilbert problem formulation and the method of analytical continuation. It shows that the stress field exhibits $\rho^{-\frac{1}{2}+i\beta}$ singularities near the inclusion tips which are exactly the same as the case of a line inclusion problem. Numerical examples of composite materials under remote uniform load or concentrated force are considered. There are several remarks on these numerical results. In general, the magnitude of the tractions along the interface increases with the rigidity of the fiber. Furthermore, the strength of a positively singular traction on the inclusion surface is always higher than that on the bonded interface which suggests that either matrix or fiber splitting along the inclusion surface, depending on the loading conditions, would be a dominate failure mode, as considered in the present study. Finally, the oscillatory behavior in tractions around the inclusion tip is discussed and found to be negligible from the classical continuum mechanics points of view.

References

[1]Mura, T., "Inclusion Problems," *Applied Mechanics Reviews*, Vol. 41, No. 1, 1988, pp. 15–20.

[2]Eshelby, J. D., "The Determination of the Elastic Field of an Ellipsoidal Inclusion and Related Problems," *Proceedings of the Royal Society*, Vol. 241, 1957, pp. 376–396.

[3]Muskhelishvili, N. I., *Some Basic Problems of Mathematical Theory of Elasticity*, Noordhoff, Groningen, The Netherlands, 1953.

[4]Wang, Z. Y., Zhang, H. T., and Chou, Y. T., "Characteristics of the Elastic Field of Rigid Line Inhomogeneity," *Journal of Applied Mechanics*, Vol. 52, 1985, pp. 818–822.

[5]Erdogan, F., and Gupta, G. D., "Stress Near a Flat Inclusion in Bonded

Dissimilar Material," *International Journal of Solids Structures*, Vol. 8, 1972, pp. 533–547.

[6]Atkinson, C., "Some Ribbon-Like Inclusion Problems," *International Journal of Engineering Science*, Vol. 11. 1973, pp. 243–266.

[7]Ballarini, R., "An Integral Equation Approach for Rigid Line Inhomogeneity Problems," *International Journal of Fracture*, Vol. 33, 1987, pp. R23–R26.

[8]Stroh, A. N., "Dislocations and Cracks in Anisotropic Elasticity," *Philosophical Magazine*, Vol. 7, 1958, pp. 625–646.

[9]Li, Q., and Ting, T. C., "Line Inclusions in Anisotropic Elastic Solid," *Journal of Applied Mechanics*, Vol. 56, 1989, pp. 556–563.

[10]Wu, K. C., "Line Inclusions at Anisotropic Bimaterial Interface," *Mechanics of Materials*, Vol. 10, 1990, pp. 173–182.

[11]Chao, C. K., and Shen, M. H., Explicit Solution for Elastic and Thermoelastic Fields with a Rigid Circular-Arc Inclusion," *International Journal of Fracture,* Vol. 65, 1994, pp. 1–18.

[12]Ballarini, R., "A Rigid Line Inclusion at Bimaterial Interface," *Engineering Fracture Mechanics*, Vol. 37, 1990, pp. 1–5.